Landau-Ginzburg model for antiferroelectric phase transitions based on microscopic symmetry

Richard A. Hatt
Materials Research Laboratory, The Pennsylvania State University, University Park, Pennsylvania 16802

Wenwu Cao
Materials Research Laboratory and Department of Mathematics, The Pennsylvania State University, University Park, Pennsylvania 16802

(Received 15 February 2000)

The only Landau-type model for antiferroelectric phase transitions was proposed by Kittel, in which two interpenetrating sublattices with opposite polarizations of equal amplitude were assumed. The theory, however, did not include any mechanism to specify the relative spatial positions of the two sublattices, and therefore could not address the cell doubling during antiferroelectric phase transitions. We propose a Landau-Ginzburg-type model based on microscopic symmetry and group theory, which can, without having to assume sublattices, account for all aspects of antiferroelectric states, including local dipole orientation and cell doubling. The average of these dipoles naturally leads to the Kittel model. The inclusion of gradient terms in the free energy allows the modeling of multidomain structures and domain walls in antiferroelectric states.

INTRODUCTION

Kittel[1] proposed a macroscopic Landau-type model for the antiferroelectric (AFE) state by introducing two interpenetrating sublattices with opposite polarizations. His model describes a second-order transition from the paraelectric state to the antiferroelectric state, by truncating the free energy at the fourth order:

$$F=\alpha_1(P_1^2+P_2^2)+\alpha_2 P_1 P_2+\alpha_{11}(P_1^4+P_2^4), \qquad (1)$$

where P_1 and P_2 are the polarizations of the sublattices. If $\alpha_2>0$, the transition will favor P_1 and P_2 being antiparallel, making the low-temperature phase antiferroelectric. On the other hand, if $\alpha_2<0$, the transition will favor P_1 and P_2 being parallel, and the transition will lead to a ferroelectric state.[1–2]

This model has the intrinsic limitation that it contains only local interactions. In other words, there is no mechanism to fix the spatial relationship between the two sublattice polarizations within the crystal. This local model creates uncertainty in the antiferroelectric state. For example, the sublattice polarizations P_1 and P_2 are assumed at the same location in space (or can be anywhere in space), which leads to the cancellation of P_1 and P_2. Such a situation does not fully describe the antiferroelectric state in which adjacent primitive cells acquire opposite dipole moments and the local polarization at any space point is actually nonzero. Using group-theoretical techniques, we propose a continuum model for the antiferroelectric state built upon microscopic symmetry. The symmetry allowed distortions associated with the soft mode are given in our model, which accounts for the formation of antiparallel dipoles in adjacent cells. The free energy has also been expanded to include gradient terms of the order parameter so that multidomain structures, such as orientation twins and antiphase walls, can be modeled using the same formulation. Specifically, in this paper we will use ammonium dihydrogen phosphate $(NH_4)H_2(PO_4)$ (commonly referred to as ADP) as a prototype system to illustrate the procedure and the characteristics of the antiferroelectric phase transition.

ANTIFERROELECTRIC PHASE TRANSITION

The high-temperature phase of ADP is tetragonal with space group $I\bar{4}2d$.[3–6] Following the notation of the *International Tables for Crystallography*,[7] the conventional (nonprimitive) unit cell contains four formula units. Two of the formula units are in the primitive cell while the other two are related by the centering translation $(\frac{1}{2}\frac{1}{2}\frac{1}{2})$. At $T_C\approx -125\,^{\circ}\mathrm{C}$, the material undergoes an antiferroelectric transition to an orthorhombic phase with space group $P2_12_12_1$.[6,8] The transition is driven by a zone-boundary *M*-point soft mode and results in ionic displacements that create one dipole moment in each formula unit (four dipoles per AFE unit cell) as shown in Fig. 1. These dipole moments form a net antiferroelectric polarization along the [100] or [010] of the parent phase. This means that the fourfold rotational inversion axis of the parent paraelectric phase is lost during the transition, which leads to two rotationally related, energetically equivalent orientation domain states in the low-temperature phase. Moreover, the transition causes a primitive-cell doubling (equivalently, the centering point in the conventional parent cell is lost), leading to two additional

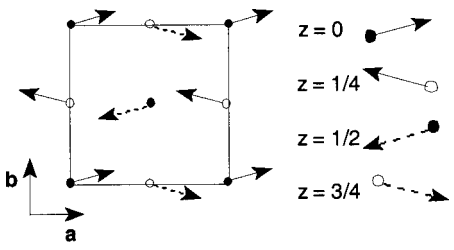

FIG. 1. Dipoles formed in the antiferroelectric phase of ADP in a conventional cell. The lattice displacement pattern can be generated from group theory.

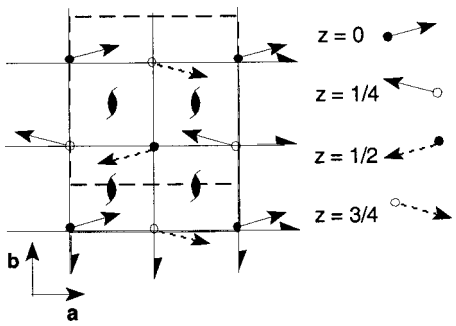

FIG. 2. Microscopic positions of the symmetry elements, creating the antiferroelectric polarization. The AFE unit cell is shown by the dashed line, with origin at $(0, \frac{1}{4}, \frac{3}{8})$. The screw axes parallel to **a** are at $z=\frac{3}{8}$, and the screw axes parallel to **b** are at $z=\frac{1}{4}$.

antiphase states that are translationally related to the two orientation states. Overall, there are four possible domains in the AFE state of ADP.

GROUP THEORETICAL DESCRIPTION OF THE TRANSITION

Once the structures and space groups of the high- and low-temperature phases have been determined, the microscopic positions of the symmetry elements are fixed (we will use the settings of Ref. 7), as shown in Fig. 2. Specifically, we note that the three mutually perpendicular twofold screw axes in the AFE phase do not allow a net dipole moment for the unit cell of the low-temperature phase, although they do allow antiferrolectric polarizations.

The *M*-point soft mode driving the transition in ADP may be described by the physically irreducible M_3M_4 representation,[4] which is simply the direct sum $M_3 \oplus M_3^*$ (here we use the labeling of Miller and Love[9]). This representation carries a two-component order parameter (OP), (p_1,p_2), whose values are listed in Table I. Physically, the OP corresponds to the molecular dipole moments within the **a**-**b** plane; p_1 represents the component along the **a** direction, and p_2 represents the component along the **b** direction. This OP is a continuum field, which is equal to the dipole moment at the sites of each formula unit.

Knowing the irreducible representation allows the lattice distortions that arise in the transition to be calculated using the ISOTROPY[10] software package. For simplicity we will restrict our discussion to distortions arising at Wyckoff **a** sites only, which are listed in Table II. These distortions can be used to construct the dipole arrangement within the low-temperature unit cell. As an example, consider the distortions that arise in domain S_1, for which the OP is $(p_1,p_2)=(p_a,p_b)$. If $p_a>p_b$, the distortions result in the configuration shown in Fig. 1, which agree well with the observed dipolar distribution by Blinc *et al.*[8]

TABLE I. Values of the order parameter for different domain states.

Domain	Order parameter
S_1	(p_a,p_b)
S_2	$(p_b,-p_a)$
S_3	$(-p_a,-p_b)$
S_4	$(-p_b,p_a)$

TABLE II. Group theoretically allowed distortions at Wyckoff **a** sites in domain S_1.

Position	Distortions	Relationship to (0,0,0) site
(0,0,0)	$p_a(1,0,0)+p_b(0,-1,0)$	$\{E\|000\}$
$(\frac{1}{2},\frac{1}{2},\frac{1}{2})$	$p_a(-1,0,0)+p_b(0,1,0)$	$\{C_{2z}\|\frac{1}{2}\,\frac{1}{2}\,\frac{1}{2}\}$
$(0,\frac{1}{2},\frac{1}{4})$	$p_a(-1,0,0)+p_b(0,-1,0)$	$\{C_{2y}\|\frac{1}{2}\;1\;\frac{3}{4}\}$
$(\frac{1}{2},1,\frac{3}{4})$	$p_a(1,0,0)+p_b(0,1,0)$	$\{C_{2x}\|\frac{1}{2}\;1\;\frac{3}{4}\}$

Figure 1 was constructed based only on the microscopic positioning of the symmetry elements and the allowed distortions from group theoretical considerations, as in Fig. 2. For example, a dipole moment at position (0, 0, 0) necessarily means, by action of the screw axis parallel to the *z* axis, an oppositely directed dipole moment at the parent cell centering point of $(\frac{1}{2}\frac{1}{2}\frac{1}{2})$. The screw axis parallel to the *x* axis further implies, from these two dipoles, that the other two antialigned dipoles within the AFE unit cell must be present. Hence, there is no need for defining sublattices and no need to explain why such sublattices would adopt exactly equal magnitudes but opposite orientation. More importantly, the spatial relationship between the two sublattices naturally comes out of our model. If a single dipole moment is formed within a parent formula unit, one can generate its counterparts by symmetry requirements to form the antiferroelectric polarization of the whole unit cell of the low-temperature phase. Also, since the dipole moment at the centering point $(\frac{1}{2}\frac{1}{2}\frac{1}{2})$ is opposite to the dipole moment at (0,0,0), the doubling of the unit cell size is naturally explained.

HYSTERESIS AND THE RELATION TO THE SUBLATTICES PROPOSED BY KITTEL

A well-known characteristic of antiferroelectrics is the double hysteresis loop, as shown in Fig. 3. In the one-dimensional antiferroelectric model proposed by Kittel, there is no net polarization. However, if an external electric field is applied, the sublattice polarization parallel to the field grows and the other sublattice polarization opposite to the field shrinks, resulting in a net polarization. When the field strength becomes sufficiently large, the polarization in the direction opposite to the field abruptly switches orientation to become parallel to the field, resulting in a ferroelectric state. Because of symmetry constraints, a double hysteresis

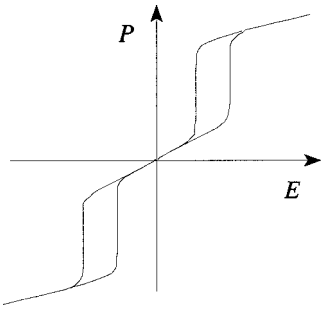

FIG. 3. Double hysteresis loop, a characteristic of the antiferroelectric state.

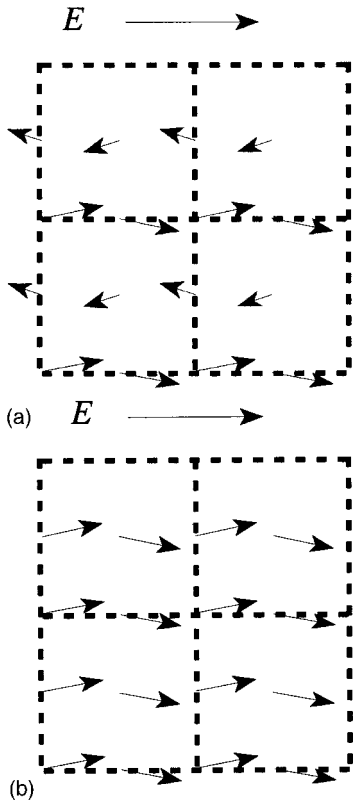

FIG. 4. Molecular dipole moments in the presence of an external electric field, (a) before switching and (b) after switching.

will be produced during such a switching process.[2]

In our model, we describe the hysteresis in terms of the dipole moments associated with each of the four formula units in an AFE unit cell. Consider an external electric field applied to domain S_1, parallel to the **+a** direction. This field will interact with the dipoles, causing $p_a>0$ to increase in magnitude and $p_a<0$ to decrease in magnitude, as shown in Fig. 4(a). Note that p_b is not affected in our model. At sufficiently large field strength, the dipoles with p_a antiparallel to the external field will flip so that p_a becomes parallel to **+a**, as shown in Fig. 4(b). This results in a state in which the dipole components are parallel along the **a** direction and antiparallel along the **b** direction. It is a ferroelectric state with the polarization along **a**, but with a cell size twice that of the Kittel model.

In order to make the connection between our microscopic model and the Kittel macroscopic model, we use the definition of the polarization, which is an average of molecular dipole moments over a given volume $P=(1/V)\Sigma p_i$. The sublattice polarizations P_1 and P_2 in the Kittel one-dimensional model can then be defined, in terms of the molecular dipole moments in our model, as

$$P_1=\frac{1}{V}\sum_{i\ (p_a>0)} p_{ai}, \quad P_2=\frac{1}{V}\sum_{i\ (p_a<0)} p_{ai}. \tag{2}$$

In other words, in the AFE state the formula units containing a positive dipole-moment component in the **a** direction form one sublattice with polarization P_1, and the formula units containing a negative dipole-moment component in the **a** direction form the other sublattice with polarization P_2. The difference between the microscopic theory presented here and macroscopic continuum theory of Kittel is that the latter cannot provide the spatial relationships among dipoles of adjacent cells, and cannot account for the dipole tilt which occurs in the ADP system.

TABLE III. Invariants for the antiferroelectric transition driven by a soft mode corresponding to the M_3M_4 irreducible representation.

$\phi^{(2)}=p_1^2+p_2^2$	$\delta_1=\left(\frac{\partial p_1}{\partial x}\right)^2+\left(\frac{\partial p_2}{\partial y}\right)^2$
$\phi_1^{(4)}=(p_1^2+p_2^2)^2$	$\delta_2=\frac{\partial p_1}{\partial x}\frac{\partial p_2}{\partial x}-\frac{\partial p_1}{\partial y}\frac{\partial p_2}{\partial y}$
$\phi_2^{(4)}=p_1^4+p_2^4$	$\delta_3=\left(\frac{\partial p_1}{\partial y}\right)^2+\left(\frac{\partial p_2}{\partial x}\right)^2$
$\phi_3^{(4)}=p_1^3p_2-p_1p_2^3$	

LANDAU-GINZBURG FREE ENERGY BASED ON MICROSCOPIC SYMMETRY

Adding OP gradient terms to the free energy, i.e., using the Landau-Ginzburg-type free energy, will allow us to describe inhomogeneous structures, such as orientational twins and antiphase walls. The invariant polynomials of the OP and its derivatives can also be obtained using the ISOTROPY program. In this paper, we have truncated the free energy at the fourth power of the OP to limit our discussions to a second-order transition. We also assume that the OP field varies slowly in space so that only the first derivatives of the OP are included in the free energy. We write

$$F=A\varphi^{(2)}+B_i\varphi_i^{(4)}+D_i\delta_i \quad (i=1,2,3), \tag{3}$$

where the invariant polynomials $\varphi^{(2)}$, $\varphi_i^{(4)}$, and δ_i are given in Table III. The coefficients $A=A_0(T-T_c)$, B_i, and D_i are constants.

For single domain states, all derivatives of the OP must vanish; i.e., $\delta_i=0$. Considering the single domain state S_1, the two component OP is (p_a,p_b) with both p_a and p_b nonzero. Since the symmetry of the low-temperature phase is known, the ionic displacements and dipole moments in each unit cell can be determined experimentally from neutron scattering. In other words, the ratio of the amplitudes $\kappa=p_a/p_b$ can be measured in the antiferroelectric state

$$p_b=\kappa p_a. \tag{4}$$

Because all derivatives of the OP vanished in the single domain state, energy minimization of Eq. (3) leads to

$$\left.\frac{\partial F}{\partial p_1}\right|_{p=(p_a,\kappa p_a)}=2Ap_a+[4B_1(l+\kappa^2)+4B_2+B_3(3\kappa-\kappa^3)]p_a^3=0, \tag{5a}$$

$$\left.\frac{\partial F}{\partial p_2}\right|_{p=(p_a,\kappa p_a)} = 2A\kappa p_a + \left[4B_1(1+\kappa^2) + 4B_2\kappa^2 + B_3\left(\frac{1}{\kappa} - 3\kappa\right)\right]\kappa p_a^3 = 0. \tag{5b}$$

In order for Eqs. (5a) and (5b) to give the same solution for p_a, the sum involving the B_2 and B_3 terms must be equal,

$$4B_2 + B_3(3\kappa - \kappa^3) = 4B_2\kappa^2 + B_3\left(\frac{1}{\kappa} - 3\kappa\right), \tag{6}$$

which can be written as a fourth-degree polynomial equation in κ:

$$\kappa^4 + b\kappa^3 - 6\kappa^2 - b\kappa + 1 = 0 \tag{7}$$

with $b = 4B_2/B_3$. This equation has four roots,

$$\left(\kappa_1, -\frac{1}{\kappa_1}, \kappa_2, -\frac{1}{\kappa_2}\right), \tag{8}$$

where

$$\kappa_1 = -\frac{b}{4} - \frac{1}{4}\sqrt{16+b^2} + \frac{1}{2\sqrt{2}}(16+b^2)^{1/4}\sqrt{b+\sqrt{16+b^2}}, \tag{9a}$$

$$\kappa_2 = -\frac{b}{4} + \frac{1}{4}\sqrt{16+b^2} + \frac{1}{2\sqrt{2}}(16+b^2)^{1/4}\sqrt{-b+\sqrt{16+b^2}}. \tag{9b}$$

One of the above solutions, Eq. (9a), will be less than 1 and greater than 0 (i.e., $0<\kappa<1$), which is the solution we seek since it corresponds to the OP in domain S_1, with $p_a > p_b$ (see Fig. 1). Because Eq. (7) does not contain any temperature-dependent terms, the solution κ will be temperature independent.

Once κ is determined, Eq. 5(a) allows the value of p_a to be determined as a function of the expansion coefficients in Eq. (3):

$$p_a^2 = \frac{-2A}{4B_1(1+\kappa^2) + 4B_2 + B_3(3\kappa - \kappa^3)}. \tag{10}$$

We note that the expansion coefficient A is temperature dependent, $A = A_0(T - T_c)$, so that the amplitude of the order parameter satisfies the universal relation for a second order phase transition, i.e.,

$$p_b \propto p_a \propto \sqrt{T_c - T}.$$

ORDER-PARAMETER PROFILES FOR TWINS AND ANTIPHASE STRUCTURES

The Landau-Ginzburg free energy, Eq. (3), allows us to describe inhomogeneous structures. We will study both orientation twins and antiphase structures in the AFE phase, each composed of two different domains separated by a domain wall. Since there are four possible domains in the AFE state, there will be $4\times4 = 16$ possible pairings of domains from which we can construct orientation twins or antiphase walls. However, using the idea of equivalence in group theory, the pairing set can be much reduced. We find three classes of two-domain structures to be considered, as listed in Table IV along with the type of structure represented (the trivial degenerate structure that has the same domain on both sides of the wall is actually a single domain structure): two orientation twins, and one antiphase structure.

TABLE IV. Equivalence classes of two-domain (twins and antiphase) structures.

Domain pair	Type	Relation to S_1
(S_1,S_2)	orientation twin	$\{\sigma_{bd}\|0\,\frac{1}{2}\,\frac{1}{4}\}$
(S_1,S_4)	orientation twin	$\{\sigma_{bd}\|\frac{1}{2}\,1\,\frac{3}{4}\}$
(S_1,S_3)	antiphase structure	$\{E\|\frac{1}{2}\,\frac{1}{2}\,\frac{1}{2}\}$

We will first consider the orientation twin formed by domains S_1 and S_2. The domain wall orientation for such a twin can be determined by strain matching,[11,12] noting that this transition belongs to the Aizu[13] species $\bar{4}2mF222$. The strain allowed domain walls are the planes $x = \pm y$ (see Fig. 5). Since properties of the crystal will change only along the direction normal to this wall, we will rotate to a new coordinate system so that x' is normal to the wall. The OP components (and any other properties of the twin) then will be functions of x' only. This means that the derivatives in the gradient part of the free energy, Eq. (3), can be rewritten as

$$\frac{\partial p}{\partial x} \to \pm\frac{1}{\sqrt{2}}\frac{\partial p}{\partial x'}, \quad \frac{\partial p}{\partial y} \to \pm\frac{1}{\sqrt{2}}\frac{\partial p}{\partial x'}. \tag{11}$$

For such a twin structure, the OP varies across the wall from its value in S_1 to its value in S_2,

$$p_1 = \begin{cases} p_a, & x' \to -\infty \\ p_b, & x' \to +\infty \end{cases}, \quad p_2 = \begin{cases} p_b, & x' \to -\infty \\ -p_a, & x' \to +\infty \end{cases}. \tag{12}$$

In order to match the boundary conditions in Eq. (12), it is convenient to change the dependent variables

$$p_1 = p_a f_1 + p_b f_2,$$
$$p_2 = p_b f_1 - p_a f_2. \tag{13}$$

Here, the functions f_1 and f_2 are normalized order-parameter components and have simpler boundary conditions

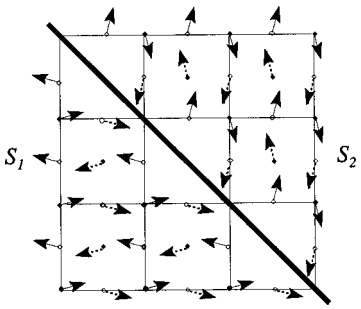

FIG. 5. Twin structure with a domain wall oriented parallel to the $(1\bar{1}0)$ lattice plane.

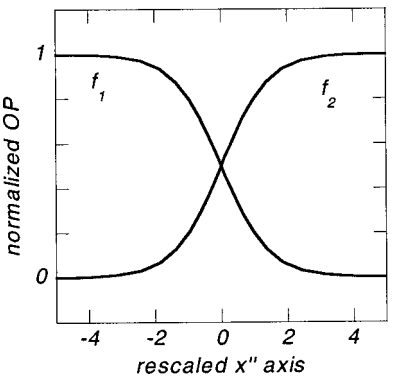

FIG. 6. Numerical solution for the order parameter profile of an orientation twin with $\gamma'=3.0$.

$$f_1=\begin{cases}1, & x'\to-\infty\\ 0, & x'\to+\infty,\end{cases}\quad f_2=\begin{cases}0, & x'\to-\infty\\ 1, & x'\to+\infty.\end{cases}\tag{14}$$

We now apply the Euler-Lagrange equations

$$\frac{d}{dx'}\frac{\partial F}{\partial f_{i,x'}}=\frac{\partial F}{\partial f_i}\quad (i=1,2)\tag{15}$$

and obtain a coupled set of ordinary differential equations

$$D\frac{d^2f_1}{dx'^2}=\alpha f_1+\beta f_1^3+\gamma f_1f_2^2,$$

$$D\frac{d^2f_2}{dx'^2}=\alpha f_2+\beta f_2^3+\gamma f_1^2f_2,\tag{16}$$

where

$$D=(1+\kappa^2)(D_1+D_3),$$

$$\alpha=(1+\kappa^2)A,\tag{17}$$

$$\beta=p_a^2[4(1+\kappa^2)^2B_1+4(1+\kappa^4)B_2+4\kappa(1-\kappa^2)B_3],$$

$$\gamma=p_a^2[4(1+\kappa^2)^2B_1+24\kappa^2B_2-12\kappa(1-\kappa^2)B_3].$$

In order to meet the boundary conditions in Eq. (14), we must have

$$\alpha+\beta=0.\tag{18}$$

The x' axis can be rescaled to

$$x''=x'\sqrt{\frac{\beta}{D}}\tag{19}$$

to arrive at a simplified set of dimensionless equations

$$\frac{d^2f_1}{dx''^2}=-f_1+f_1^3+\gamma' f_1f_2^2,$$

$$\frac{d^2f_2}{dx''^2}=-f_2+f_2^3+\gamma' f_1^2f_2,\tag{20}$$

where $\gamma'=\gamma/\beta$ is temperature independent. Equations (20) have been solved for other systems[14] and the solutions for the choice of $\gamma'=3.0$ are illustrated in Fig. 6.

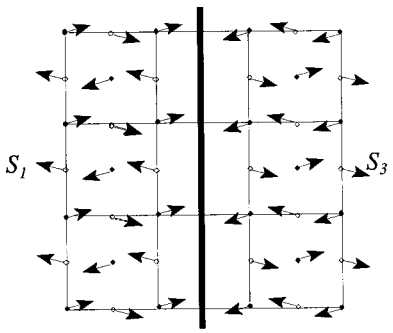

FIG. 7. Dipole arrangement in the vicinity of an antiphase wall between S_1 and S_3.

For the second type of orientation twin involving domains S_1 and S_4, the boundary conditions are

$$p_1=\begin{cases}p_a, & x'\to-\infty\\ -p_b, & x'\to+\infty,\end{cases}\quad p_2=\begin{cases}p_b, & x'\to-\infty\\ p_a, & x'\to+\infty.\end{cases}\tag{21}$$

We make the following change of variables

$$p_1=p_af_1-p_bf_2,$$

$$p_2=p_bf_1+p_af_2.\tag{22}$$

The same set of equations, Eqs. (20), for the functions f_1 and f_2 can be derived and similar solutions can be obtained.

For the antiphase structures, we cannot use the strain compatibility relations to predict the orientation of the wall since the strain compatibility relations are automatically satisfied. However, we can simplify the equations to quasi-one-dimensional using the same procedure described above. Again, we rotate the coordinate system such that x' is perpendicular to the wall. The derivatives in the gradient part of the free energy can again be expressed in terms of derivatives in the x' direction. By defining the new normalized order parameter g,

$$p_1=p_ag,\quad p_2=p_bg\tag{23}$$

and using a rescaling of the space variable similar to Eq. (19) (but dependent upon the specific orientation of the wall), we can simplify the system to a single differential equation for the function g,

$$\frac{d^2g}{dx''^2}=-g+g^3.\tag{24}$$

For the antiphase structure formed by domains S_1 and S_3 (see Fig. 7), the boundary conditions are

$$p_1=\begin{cases}-p_a, & x'\to-\infty\\ p_a, & x'\to+\infty,\end{cases}\quad p_2=\begin{cases}-p_b, & x'\to-\infty\\ p_b, & x'\to+\infty,\end{cases}\tag{25}$$

or

$$g=\begin{cases}-1, & x''\to-\infty\\ 1, & x''\to+\infty\end{cases}.\tag{26}$$

Equation (24) has the analytic solution

$$g = \tanh\left(\frac{x''}{\sqrt{2}}\right). \tag{27}$$

SUMMARY AND CONCLUSIONS

We have proposed a Landau-Ginzburg model based on microscopic symmetry to describe a second-order antiferroelectric phase transition. The OP field used is directly correlated to the local dipole moments of the formula units, instead of the macroscopically averaged polarization. Our model not only can derive the macroscopic model proposed by Kittel but also can address the dipole tilt and cell doubling in the antiferroelectric transition. There is no need to assume separate sublattices in our model.

When the antiferroelectric state is switched to a ferroelectric state by an external electric field, our model predicts a unit cell size twice as large as that of the macroscopic picture obtained from previous investigations.[2] This picture is more consistent with the microscopic picture observed experimentally that the dipoles are actually tilted from the **a** and **b** directions.

There are four domain states in the antiferroelectric phase and they form two distinct orientation twins and one type of antiphase structure. The addition of gradient energy terms in the free energy allows us to model multidomain inhomogeneous structures. Numerical solutions for the inhomogeneous OP profiles describe the gradual change of the dipole amplitude and orientation across the domain walls. We find that if, in the free energy, only the coefficient of the quadratic term is assumed to be temperature dependent, the local dipoles have a fixed orientation independent of temperature, while the amplitude of the dipole moment is a function of temperature.

ACKNOWLEDGMENTS

This work was sponsored by the Office of Naval Research under the MRUI Grant and the Grant for Piezocrystal Resource.

[1] C. Kittel, Phys. Rev. **82**, 729 (1951).
[2] L. E. Cross, J. Phys. Soc. Jpn. **23**, 77 (1967).
[3] H. Meister *et al.*, Phys. Rev. **184**, 550 (1969).
[4] H. Konwent and J. Lorenc, Phys. Status Solidi B **88**, 747 (1978).
[5] L. Tenzer, B. C. Frazer, and R. Pepinsky, Acta Crystallogr. **11**, 505 (1958).
[6] R. O. Keeling, Jr. and R. Pepinsky, Z. Kristallogr. **106**, 236 (1955).
[7] *International Tables for Crystallography*, edited by T. Hahn (Reidel, Dordrecht, 1983).
[8] R. Blinc, J. Slak, and I. Zupanĉik, J. Chem. Phys. **61**, 988 (1974).
[9] S. C. Miller and W. F. Love, *Tables of Irreducible Representations of Space Groups and Co-Representations of Magnetic Space Groups* (Pruett, Boulder, 1967).
[10] H. T. Stokes and D. M. Hatch, *Isotropy Subgroups of the 230 Crystallographic Space Groups* (World Scientific, Singapore, 1988). Internet and DOS (PC) versions of this software are available at URL http://www.physics.byu.edu/~stokesh/isotropy.html
[11] J. Sapriel, Phys. Rev. B **12**, 5128 (1975).
[12] J. Fousek and V. Janovec, J. Appl. Phys. **40**, 135 (1969).
[13] K. Aizu, J. Phys. Soc. Jpn. **27**, 387 (1969).
[14] W. Cao and G. R. Barsch, Phys. Rev. B **41**, 4334 (1990).